

## Absolute Measurement of an Optical-Rectification Coefficient in Ammonium Dihydrogen Phosphate\*

J. F. WARD†

*The Harrison M. Randall Laboratory of Physics, University of Michigan, Ann Arbor, Michigan*

(Received 17 September 1965)

A direct measurement of an optical-rectification coefficient in ammonium dihydrogen phosphate ( $\text{NH}_4\text{H}_2\text{PO}_4$ ) is described. The result is  $(X^0_{xyz} + X^0_{zyx}) = (1.32 \pm 0.18) \times 10^{-7}$  esu, at 6943 Å and 27°C. The 15% uncertainty represents an improvement by a factor of 20 over the previous absolute measurement of an optical rectification coefficient by Bass *et al.* The improved precision makes possible a more meaningful test of a theoretical relationship between the optical-rectification coefficients  $X^0$ , and the linear electro-optic coefficient  $X^\omega$ . This relationship, first pointed out by Armstrong *et al.* and studied in more detail by Ward and Franken, is  $(X^0_{ijk} + X^0_{ikj}) = \frac{1}{4}(X^\omega_{jik} + X^\omega_{kij})$ . It is concluded that the present measurement, together with electro-optic data from the literature, is consistent with the validity of this relationship.

### I. INTRODUCTION

OPTICAL rectification<sup>1-5</sup> is the production of a steady polarization  $\mathbf{p}$  in a medium that is subjected to an optical, electromagnetic field. The magnitude of the polarization is proportional to the square of the optical-electric-field amplitude. The tensor coefficient for the process  $X^0$ , is defined by

$$p_i^0 = X^0_{ijk} E_j^\omega E_k^\omega, \quad (1)$$

where superscripts indicate relevant frequencies and the convention of summation over repeated indices is adopted. Theoretical arguments relating this coefficient to the linear electro-optic coefficient were first developed by Armstrong *et al.*<sup>6</sup> and in more detail by Ward and Franken.<sup>7</sup> The linear electro-optic effect may be described by an equation similar to Eq. (1):

$$p_j^\omega = X^\omega_{jik} E_i^0 E_k^\omega, \quad (2)$$

and the relationship between the coefficients is

$$(X^0_{ijk} + X^0_{ikj}) = \frac{1}{4}(X^\omega_{jik} + X^\omega_{kij}) = \frac{1}{2}X^\omega_{jik}. \quad (3)$$

For crystals of class  $V_d$  such as ammonium dihydrogen phosphate ( $\text{NH}_4\text{H}_2\text{PO}_4$ ) and potassium dihydrogen phosphate ( $\text{KH}_2\text{PO}_4$ ), Eq. (3) reduces to two relationships

$$(X^0_{xyz} + X^0_{zxy}) = \frac{1}{4}(X^\omega_{yxz} + X^\omega_{zxy}), \quad (4a)$$

and

$$(X^0_{zxy} + X^0_{zyx}) = \frac{1}{4}(X^\omega_{xzy} + X^\omega_{yzx}). \quad (4b)$$

\* This work was supported in part by the U. S. Atomic Energy Commission.

† Permanent address: Clarendon Laboratory, Oxford University, Oxford, England.

<sup>1</sup> M. Bass, P. A. Franken, J. F. Ward, and G. Weinreich, *Phys. Rev. Letters* **9**, 446 (1962).

<sup>2</sup> M. Bass, P. A. Franken, and J. F. Ward, *Bull. Am. Phys. Soc.* **8**, 624 (1963).

<sup>3</sup> M. Bass, Ph.D. thesis, University of Michigan, 1964 (unpublished).

<sup>4</sup> M. Subramanian, Ph.D. thesis, Purdue University, 1964 (unpublished).

<sup>5</sup> M. Bass, P. A. Franken, and J. F. Ward, *Phys. Rev.* **138**, A534 (1965).

<sup>6</sup> J. A. Armstrong, N. Bloembergen, J. Ducuing, and P. S. Pershan, *Phys. Rev.* **127**, 1918 (1962).

<sup>7</sup> J. F. Ward and P. A. Franken, *Phys. Rev.* **133**, A183 (1964).

The electro-optic coefficients for each of the crystals mentioned above are available in the literature. Bass *et al.*<sup>5</sup> have measured  $(X^0_{zxy} + X^0_{zyx})$  in  $\text{KH}_2\text{PO}_4$  to within a factor of 3, which large uncertainty arises mainly from the measurement of optical power. The result is consistent with Eq. (4b). Measurements of the variation of coefficients with temperature and relative measurements in various crystals<sup>5</sup> have indirectly supported the validity of Eq. (3).

The present work is concerned with a direct verification of Eq. (3) to improved precision. In particular,  $(X^0_{xyz} + X^0_{zxy})$  in  $\text{NH}_4\text{H}_2\text{PO}_4$  is measured to test Eq. (4a).

### II. EXPERIMENTAL

The experimental arrangement is shown in Fig. 1. Light from a Q-switched ruby laser propagates through an  $\text{NH}_4\text{H}_2\text{PO}_4$  crystal and into a calorimeter. The crystal forms the dielectric of a parallel plate capacitor across which a voltage is induced by the polarization set up in the crystal. The optical rectification coefficient is proportional to the time integral of this voltage divided by the optical energy measured by the calorimeter. The detailed relationship is derived in Sec. III.

#### 1. Light Source

As the coefficient is small, a high-power light source is required. We have used a Q-switched ruby laser (LSI-Laser Systems Center LS 100). For run I a rotating prism Q switch was used to produce single pulses with energies 15–30 mJ and full width at half-intensity

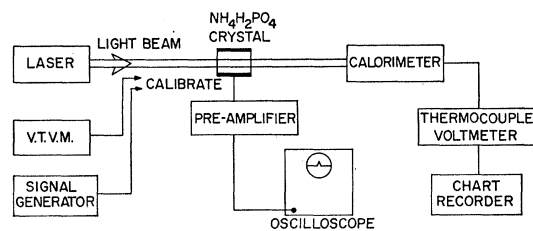


FIG. 1. Schematic diagram of the apparatus.

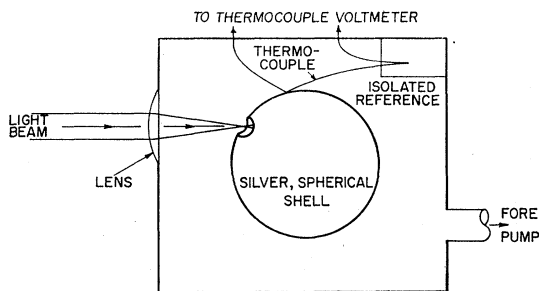


FIG. 2. Schematic diagram of the calorimeter designed and constructed by C. W. Bruce of the U. S. Air Force Weapons Laboratory.

$25 \pm 5$  nsec. For runs II, III, and IV a uranyl glass saturable filter was inserted within the laser cavity to produce single pulses with energies 50–110 mJ and full width at half-intensity  $15 \pm 3$  nsec.

## 2. Calorimeter

The calorimeter<sup>8</sup> which has been fundamental to the improved precision of this measurement was designed and constructed by Bruce of the U. S. Air Force Weapons Laboratory. Figure 2 indicates the design. The light is focused at the small entrance hole in a silver, spherical shell. The defocused beam hits the inside of the shell and is absorbed uniformly at the inner surface over many reflections. The rise in temperature is measured with a thermocouple whose emf is displayed on a chart recorder. Maximum voltage is recorded within 4 sec of the optical pulse and the decay-time constant is 2 min. These characteristics are achieved by minimizing the mass of the shell and thermally isolating it within an evacuated enclosure. Thermal loss is compensated by extrapolating the thermocouple voltage back to the time at which the optical pulse occurs. A more detailed description of the calorimeter is given in Ref. 8.

## 3. Crystal

The crystal geometry is shown in Fig. 3. This, and the choice of  $\text{NH}_4\text{H}_2\text{PO}_4$ , were dictated by the relatively large size of the optical rectification coefficient which is measured. Another advantage stems from the smallness of the piezoelectric coefficient  $d_{14}$ , which relates the voltage induced across the crystal capacitor to a strain in the direction of the light beam. This is relevant to the size of a piezoelectric signal which is seen after each light pulse. The signal is predominantly at the fundamental acoustic resonant frequency of the crystal ( $\sim 60$ kcps) and, in the present case, its maximum amplitude is only a few percent of the peak optical-rectification signal. The phenomenon is interpreted<sup>8</sup> as being due to a small absorption of laser light by the crystal followed by impulsive thermal expansion. In

<sup>8</sup> C. W. Bruce, U. S. Air Force Weapons Laboratory Technical Report No. 64-127, 1965 (unpublished).

previous work with  $\text{KH}_2\text{PO}_4$ ,<sup>3</sup> the peak-to-peak piezoelectric signal was larger than the peak optical-rectification signal, and although the former increases more slowly than the latter it gave rise to a significant distortion of the optical-rectification signal. No significant distortion occurs in the present experiment.

Silver electrodes are painted directly on two crystal surfaces. In previous work<sup>3,5</sup> brass electrodes were held approximately 0.005 cm from the crystal surfaces to prevent laser light from striking the electrodes. This reduced a spurious signal, thought to arise from photoelectric emission from the electrodes, but introduced an uncertainty into the results because of the capacitance of the crystal-electrode gap. In the present work, the optical-rectification signal has been increased by the choice of crystal and geometry so that spurious signals are small in comparison and we prefer to eliminate the gap and the uncertainty arising from it.

The experiment is insensitive to geometrical alignment errors. The capacitor plates are oriented to within  $1^\circ$  with respect to the crystal axes. The direction of propagation of the light and the plane of polarization are aligned to within  $3^\circ$  with respect to the crystal axes. The combined error in the magnitude of the optical rectification coefficient from these sources is less than  $\frac{1}{2}\%$ .

## 4. Signal Detector

An equivalent circuit for the crystal considered as a generator is shown in Fig. 4. The open-circuit generator voltage is proportional to the instantaneous light intensity, the constant for the present crystal geometry being about 24 mV/MW. We have used optical pulses with peak power in the range 0.5–7 MW which result in peak optical-rectification signals of 12–170 mV. The method chosen for integrating this voltage over the pulse time is to display the voltage as faithfully as possible on an oscilloscope and to photograph, cut out, and weigh the area under the trace. The uncertainty introduced by this technique is small compared with other contributions to the uncertainty of the optical-rectification coefficient (see Sec. III).

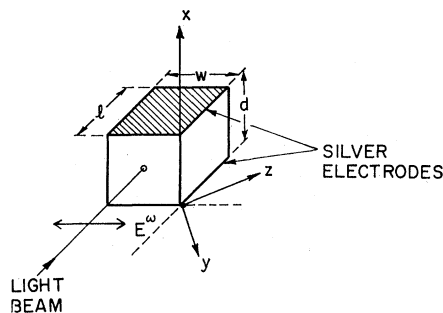
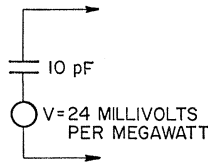


FIG. 3. The cut of crystal used. Approximate crystal dimensions are  $w=d=1$  cm,  $l=2$  cm. The light beam is in the  $yz$  plane at  $45^\circ$  to the  $y$  and  $z$  axes and the optical electric vector lies in the  $yz$  plane. Silver electrodes are painted on the two  $yz$  plane surfaces of the crystal.

FIG. 4. Equivalent circuit of the crystal considered as a generator with voltage proportional to the power of the light beam in the crystal.



The detector response time is not negligible compared to times characteristic of the optical pulse, which necessitates a small ( $< 2\%$ ) correction that is now estimated. The detector response may be approximated by that of a low-pass  $RC$  circuit with  $RC \equiv \tau$ . The indicated voltage  $v$  is related to the true signal voltage  $V$  by

$$v + \tau (dv/dt) = V. \quad (5)$$

If the pulse lasts from  $-t_0$  to  $+t_0$  we have

$$v(-t_0) = V(-t_0) = V(+t_0) = 0, \quad (6)$$

so that for a time of observation  $T > t_0$

$$\int_{-t_0}^T v dt + \tau v(T) = \int_{-t_0}^{+t_0} V dt. \quad (7)$$

These terms are the observed integral, the error, and the required integral, respectively; so that a correction factor  $\alpha$  may be defined by

$$\int_{-t_0}^{+t_0} V dt \equiv \alpha \int_{-t_0}^T v dt, \quad (8)$$

where

$$\alpha - 1 = \tau v(T) / \int_{-t_0}^T v dt \approx \tau v(T) / t_0 v_{\max}. \quad (9)$$

If the integration is extended until  $v(T)$  is negligible, no error is introduced by the detector response. In practice, the integration is truncated at a time  $T$  such that  $v(T)$  is about  $2\%$  of  $v_{\max}$ . We approximate  $t_0$  by the pulse full width at half-intensity.  $\alpha - 1$  is always less than  $2\%$  and is tabulated in Table I.

Another possible source of error in the integration procedure arises because the baseline of the optical-rectification trace is shifted downward during the pulse by about  $10\%$  of the signal amplitude. This is thought to be associated with the piezoelectric and photoelectric voltages discussed in Sec. II.3. The integration procedure is appropriate if the spurious signal increases linearly during the pulse and reasonable deviations

TABLE I. Integration correction.  $\tau$  is the detector rise time,  $t_0$  the full width of the laser pulse at half-intensity, and  $\alpha$  the integration correction factor.

Run	$\tau$ (nsec)	$t_0$ (nsec)	$\alpha$
I	18	$25 \pm 5$	$1.015 \pm 0.015$
II, III, and IV	7	$15 \pm 3$	$1.01 \pm 0.01$

TABLE II. Summary of detector characteristics.

	Run	$R_{in}$ ( $\Omega$ )	$C_{in}$ (pF)	$R_{out}$ ( $\Omega$ )	Gain	Rise time (nsec)
Preamplifier	I	100K	10	70	0.3	7
	II, III, and IV	100K	4	50	0.5	2
Oscilloscope	I	Type Tektronix 551			Sensi- tivity (mV/cm)	Rise time (nsec)
		Type L Plug-in Tektronix 517		50	7	

from this are covered by the  $\pm 5\%$  error shown in Table IV.

The detector consists of a transistorized, impedance-matching preamplifier located at the crystal and an oscilloscope. One detector was used for run I and another for runs II, III, and IV. Their characteristics are summarized in Table II.

A typical trace obtained during run II is shown in Fig. 5. The signal to noise ratio, excluding the change in baseline, is better than 100:1. The improvement over earlier work<sup>5</sup> is due to greater laser power, the choice of crystal, and improvements in geometry and electronics.

Direct,  $RC$  integration, using the Tektronix 551 oscilloscope and no preamplifier, is marginally possible with the most energetic light pulses used. The results are consistent with, but less precise than, those obtained with the apparatus and procedure described above.

### 5. Calibration of the Detector

A sinusoidal voltage from a signal generator is developed across a  $50\text{-}\Omega$  resistor in series with the crystal. It is clear from the equivalent circuit of the crystal generator (Fig. 4) that a signal injected in this way, directly simulates the open circuit optical rectification signal. A factor  $\beta$  which is the ratio of the voltage across the  $50\text{-}\Omega$  resistor to that indicated at the signal generator is established by measuring the former directly with a Hewlett-Packard type-410B vacuum-tube voltmeter. The frequency selected is in the low-frequency, flat-response region for the detector (10 Mc/sec for run I, 20 Mc/sec for runs II, III, and IV.) The reduced gain for the high-frequency components of the pulse does not introduce a significant uncertainty and is taken into account by the factor  $\alpha$  discussed in Sec. II.4. Half-period areas are cut from a photograph of the oscillo-

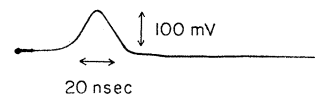


FIG. 5. Photograph of a typical optical-rectification oscilloscope trace from run II. The pulse height is 120 mV and the full width at half-height is 18 nsec.

TABLE III. Experimental data. The calorimeter thermocouple voltage  $W'$  (proportional to optical energy) and the mass of the photographed optical rectification trace  $\int_{\text{pulse}} v dt$  in mg is shown for each pulse. The detector calibration and the integration correction  $\alpha$  are discussed in Secs. II.5 and II.4, respectively. Pulses marked with an asterisk are rejected, as the laser has a tendency to produce double pulses under these conditions. The error quoted with the mean for each run of  $\int_{\text{pulse}} V dt/W'$  is deduced from scatter within the run, whereas the error quoted with the weighted means includes contributions from the calibration and integration correction factors.

Run pulse	$W'$ $\mu V$	$\int_{\text{pulse}} v dt$ (mg)	Calibration			$\int_{\text{pulse}} V dt/W'$ in V nsec/ $\mu V$	
			$\frac{V \text{ nsec}}{\text{mg}}$	$\beta$	$\alpha$	Run means	Weighted means
I.1	0.248	8.7				3.07	
I.2	0.276	9.6	0.0863	1.00	1.015	3.05	
I.3	0.254	9.3	$\pm 0.0060$	$\pm 0.07$	$\pm 0.015$	3.21	3.03
I.4	0.171	5.9				3.02	$\pm 0.06$
I.5	0.179	5.8				2.84	$\pm 0.31$
II.1*	1.53	27.5				3.05*	
II.2*	1.67	25.3				2.57*	
II.3*	1.59	24.9				2.66*	
II.4*	1.38	23.6				2.91*	
II.5	1.06	19.2	0.180			3.08	3.14
II.6	1.06	18.95	$\pm 0.005$			3.04	$\pm 0.05$
II.7	0.93	16.4				3.00	3.19
II.8	0.96	18.4				3.26	$\pm 0.23$
II.9	0.92	17.2		0.93	1.01	3.18	
II.10	0.51	9.8		$\pm 0.06$	$\pm 0.01$	3.27	
III.1	0.613	18.0				3.52	
III.2	0.519	15.15	0.127			3.50	3.30
III.3	0.621	16.8	$\pm 0.003$			3.24	$\pm 0.13$
III.4	0.499	12.3				2.96	
IV.1*	1.53	25.7	0.169			2.68*	
IV.2*	1.51	26.85	$\pm 0.004$			2.80*	

scope trace and weighed. This gives the mass corresponding to a known, time-integrated voltage which is the required calibration.

### III. ANALYSIS OF DATA

We first derive an expression for the optical-rectification coefficient in terms of measured quantities. The large dc dielectric constant  $\epsilon_x$  and the geometry of the crystal capacitor (capitance  $C$ ) allow it to be treated, to a good approximation, as a section of an infinite parallel-plane capacitor so that

$$C = \epsilon_x w l / 4\pi d, \quad (10)$$

where  $w$ ,  $l$ ,  $d$ , are crystal dimensions (see Fig. 3). In this approximation it can be shown<sup>3</sup> that the open-circuit voltage  $V$  induced across the capacitor is independent of the distribution of dipole moment within the crystal and is given by

$$V = p_x^0 A l / C d, \quad (11)$$

where  $A$  is the cross-sectional area of the light beam.

Equation (1) restricted by the symmetry of the crystal yields

$$p_x^0 = (X^0_{xyz} + X^0_{xzy}) E_y^\omega E_z^\omega. \quad (12)$$

The optical power  $P$  within the crystal is given by

$$P = E_y^\omega E_z^\omega \times n_e c A / 4\pi, \quad (13)$$

where  $c$  is the velocity of light and  $n_e$  is the extraordinary refractive index of the crystal. Equations (10),

(11), (12), and (13) yield

$$(X^0_{xyz} + X^0_{xzy}) = (c/16\pi^2) n_e \epsilon_x w (V/P). \quad (14)$$

The energy  $W$  measured by the calorimeter is

$$W = \eta \int_{\text{pulse}} P dt, \quad (15)$$

so that

$$(X^0_{xyz} + X^0_{xzy}) = \left( \frac{c}{16\pi^2} \right) n_e \epsilon_x w \eta \int_{\text{pulse}} V dt / W. \quad (16)$$

The factor  $\eta$  takes into account Fresnel reflection and scattering at the back surface of the crystal and reflection at the two surfaces of the calorimeter lens. The light reflected at the crystal surface contributes to optical rectification; all other scattered and reflected light is lost from the system. The fraction of the incident energy reflected at each lens surface is  $R'$  (taken as 5%,<sup>8</sup> the fraction reflected at the crystal surface is  $R$  (taken as 3.7%), and that scattered at the crystal surface is  $S$  (taken as  $2.5 \pm 2.5\%$ ). With these assignments

$$\eta = (1 - R - S)(1 - R')^2 / (1 + R) = 0.82 \pm 0.04. \quad (17)$$

Each laser pulse produces a pair of data: the thermocouple voltage  $W'$  (proportional to the pulse energy), and the mass of the optical rectification trace (proportional to  $\int_{\text{pulse}} v dt$ ). These data are shown in Table III together with calibration factors (Sec. II.5) and the integration correction factor  $\alpha$  (Sec. II.4 and

Table I). Table III also shows values of  $\int_{\text{pulse}} V dt/W'$  for each pulse, weighted means, and standard errors.

The pulses marked with an asterisk are rejected as, under these conditions, the laser has an intermittent tendency to produce a small second pulse carrying about 10% of the total energy. This is recorded by the calorimeter but is too late to be conveniently recorded on the optical-rectification trace.

The mean for each run is shown with standard error deduced from the scatter within the run. The standard errors of the weighted means include the uncertainties of calibration and of the integration correction. The over-all weighted average is

$$\int_{\text{pulse}} V dt/W' = 3.13 \pm 0.19 \text{ V nsec}/\mu\text{V}. \quad (18)$$

This value is shown in Fig. 6 together with the individual values, including the rejected pulses. It is seen from the figure that there is no evidence of variation with optical power except, as expected, in the double pulsing region. Nor are there significant differences between runs II and III, on the one hand, and run I, on the other, in which different apparatus are involved. This is also apparent from a comparison of the weighted means from Table III.

Equation (16) with data from Eq. (18) and Table IV yields the result

$$(X^0_{xyz} + X^0_{zxy}) = (1.32 \pm 0.18) \times 10^{-7} \text{ esu}. \quad (19)$$

#### IV. LINEAR ELECTRO-OPTIC COEFFICIENT

The relationship between the electro-optic coefficient  $r_{41}$  given in the literature and the  $\mathbf{X}^w$  of Eq. (4a) is<sup>5</sup>

$$(X^w_{yzx} + X^w_{zxy}) = -r_{41} n_e^2 n_o^2 / 2\pi. \quad (20)$$

There are three parameters which affect the magnitude of the linear electro-optic coefficient: temperature, the frequency of the low-frequency applied electric field, and the wavelength of the applied optical field.

The temperature dependence of  $r_{41}(\text{NH}_4\text{H}_2\text{PO}_4)$  in the region of 20°C is taken as  $-0.25\%/^\circ\text{C}$ . This is the

TABLE IV. Factors and uncertainties relevant to the calculation of the optical-rectification coefficient.

Calorimeter thermocouple calibration	0.0975 ± 0.0029 J/μV
Reflection-scattering factor $\eta$	0.82 ± 0.04
Width of crystal $w$	0.95 ± 0.01 cm
dc dielectric constant $\epsilon_z$ at 27°C <sup>a</sup>	56.4 ± 0.1
Refractive indices $n_o, n_e$ <sup>b</sup>	1.520, 1.476
Thermocouple voltmeter calibration	±2%
VTVM calibration (at $\frac{1}{3}$ full scale deflection)	±9%
Base line change	±5%
Geometrical alignment errors	< ±0.5%

<sup>a</sup> R. Bechmann, *Piezoelectricity* (Her Majesty's Stationery Office, London, 1957), p. 246.

<sup>b</sup> F. Zernike, Jr., *J. Opt. Soc. Am.* **54**, 1215 (1964).

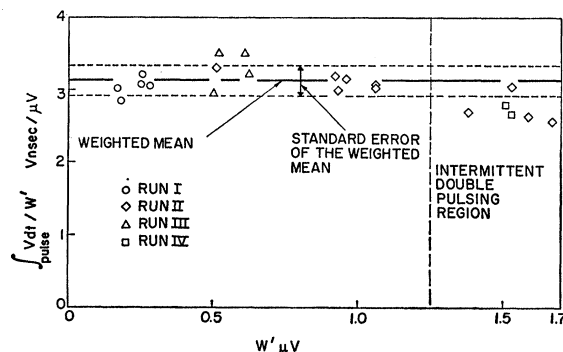


FIG. 6. The ratio of time-integrated optical-rectification signal to calorimeter thermocouple voltage (proportional to the optical-rectification coefficient) is plotted against calorimeter thermocouple voltage (proportional to optical energy) for each pulse. The weighted mean is also plotted. The high-energy pulses are rejected, as the laser has a tendency to emit a small second pulse under these conditions.

temperature dependence of the dielectric constant<sup>9</sup>  $\epsilon_x$  and is appropriate because there is experimental and theoretical evidence to show that<sup>10</sup>  $r_{mi}/(\epsilon_{ii}-1)$  or<sup>3</sup>  $r_{mi}/(\epsilon_{ii}+2)$  is essentially temperature-independent. The numerical difference between these expressions is insignificant in the present case as  $\epsilon_x$  is large.

If the frequency of the low-frequency applied field is small compared with the fundamental acoustic resonant frequency of the crystal ( $\sim 50$  kcps for crystals with 1-cm dimensions), then the *unclamped* coefficient  $r_{41}^T$  is measured. In the other limit the *clamped* coefficient  $r_{41}^S$  is measured. These are related by<sup>11</sup>

$$r_{41}^T = r_{41}^S + p_{44}d_{14}, \quad (21)$$

where<sup>12</sup>  $p_{44} = -0.051$  is an elasto-optic coefficient and  $d_{14} = -4.5 \times 10^{-8}$  esu is a piezoelectric coefficient, so that  $r_{41}^T = r_{41}^S + 0.02 \times 10^{-7}$  esu.

Inference from data on  $r_{63}(\text{KH}_2\text{PO}_4)$ <sup>13</sup> and  $r_{41}(\text{NH}_4\text{H}_2\text{PO}_4)$ <sup>14</sup> indicates that between about 5500 and 6943 Å,  $r_{41}(\text{NH}_4\text{H}_2\text{PO}_4)$  decreases by not more than 2% and we use  $1 \pm 1\%$ .

There are two values of  $r_{41}(\text{NH}_4\text{H}_2\text{PO}_4)$  in the literature: Carpenter<sup>11</sup> finds that at 22°C and 5560 Å,  $r_{41}^T = (6.25 \pm 0.10) \times 10^{-7}$  esu, and Ott and Sliker<sup>14</sup> find that at 21°C and 5460 Å,  $r_{41}^T = (7.35 \pm 0.12) \times 10^{-7}$  esu. The discrepancy between these values is unexplained. The resulting estimates for  $r_{41}^S$  at 27°C and 6943 Å, which are relevant to the comparison with the optical rectification coefficient, are  $(6.09 \pm 0.12) \times 10^{-7}$  esu and  $(7.15 \pm 0.14) \times 10^{-7}$  esu, respectively. Using

<sup>9</sup> W. P. Mason, *Phys. Rev.* **69**, 173 (1946).

<sup>10</sup> B. Zwicker and P. Sherrer, *Helv. Phys. Acta* **17**, 346 (1944).

<sup>11</sup> R. O'B. Carpenter, *J. Opt. Soc. Am.* **40**, 225 (1950).

<sup>12</sup> R. O'B. Carpenter, Ph.D. thesis, Harvard University, 1951 (unpublished), quoted by T. R. Sliker, Cleveite Corporation Engineering Memorandum No. 64-10, 1964 (unpublished).

<sup>13</sup> D. A. Berlincourt, D. R. Curran, and H. Jaffe, *Physical Acoustics*, edited by W. P. Mason (Academic Press Inc., New York, 1964), Vol. I, Part A, p. 181.

<sup>14</sup> J. H. Ott and T. R. Sliker, *J. Opt. Soc. Am.* **54**, 1442 (1964).

Eqs. (4a) and (20) gives the following predictions for the magnitude of the optical-rectification coefficient:

From Carpenter's electro-optic data,

$$(X^0_{xyz} + X^0_{xzy}) = (1.22 \pm 0.023) \times 10^{-7} \text{ esu}; \quad (22a)$$

and from Ott and Sliker's electro-optic data,

$$(X^0_{xyz} + X^0_{xzy}) = (1.43 \pm 0.026) \times 10^{-7} \text{ esu}. \quad (22b)$$

### V. CONCLUSION

The measured magnitude of an optical-rectification coefficient in  $\text{NH}_4\text{H}_2\text{PO}_4$  at  $27^\circ\text{C}$  and  $6943 \text{ \AA}$  is

$$(X^0_{xyz} + X^0_{xzy}) = (1.32 \pm 0.18) \times 10^{-7} \text{ esu}.$$

The 15% uncertainty represents an improvement by a factor of 20 over the previous absolute measurement of an optical-rectification coefficient.<sup>5</sup>

The validity of the theoretical relationship, Eq. (3), between the optical-rectification and linear electro-optic coefficients may now be tested. Magnitudes of optical-

rectification coefficients predicted from electro-optic data by Eq. (3), or more particularly, Eq. (4a), are as follows:

From Carpenter's electro-optic data,

$$(X^0_{xyz} + X^0_{xzy})_{\text{predicted}} = (1.22 \pm 0.023) \times 10^{-7} \text{ esu};$$

and from Ott and Sliker's electro-optic data,

$$(X^0_{xyz} + X^0_{xzy})_{\text{predicted}} = (1.43 \pm 0.026) \times 10^{-7} \text{ esu}.$$

The measured magnitude agrees with each of the predicted values to within experimental error. We conclude that these data are consistent with the validity of Eq. (3).

### ACKNOWLEDGMENTS

It is a pleasure to thank P. Avizonis and C. W. Bruce of the U. S. Air Force Weapons Laboratory for the loan of their calorimeter, L. Cross of LSI-Laser Systems Center for advice on the modification of the laser, and P. A. Franken for many helpful discussions.

## Theoretical Discussion of the Inverse Faraday Effect, Raman Scattering, and Related Phenomena\*

P. S. PERSHAN,† J. P. VAN DER ZIEL,‡ AND L. D. MALMSTROM

*Division of Engineering and Applied Physics, Harvard University, Cambridge, Massachusetts*

(Received 25 October 1965)

The inverse Faraday effect (IFE) occurs when circularly polarized light incident on a nonabsorbing crystal induces a magnetic moment proportional to the Verdet constant of that material, the proportionality constant being independent of the material. Some experimental details relating to the observation and proof of the IFE are presented. A microscopic, or quantum-mechanical, explanation of the IFE which also demonstrates its connection with the Faraday effect is given in terms of an optically induced "effective Hamiltonian"  $\mathcal{H}_{\text{eff}}$ . Conventional calculations of the optical constants like the Verdet constant compute optical-frequency polarizabilities for a given electronic configuration. It is shown here that these same constants are obtained by computing the average effects that optical fields have on the atomic configuration. The optically induced  $\mathcal{H}_{\text{eff}}$  is linearly dependent on the low-frequency components of  $E(t)E(t)$  and one can show the thermal average  $\langle \mathcal{H}_{\text{eff}} \rangle_{\text{thermal}}$  is equal to the temporal average  $\langle \mathbf{E}(t) \cdot \mathbf{e} \cdot (\mathbf{E}t) \rangle_{\text{time}}$ . Both the Verdet constant and the IFE coefficient arise from a thermal average of the same term in  $\mathcal{H}_{\text{eff}}$ . Similarly the Cotton-Mouton effect and its inverse arise from one other term in  $\mathcal{H}_{\text{eff}}$ . Definition of  $\mathcal{H}_{\text{eff}}$  is one technique for linearizing some nonlinear optical problems. Following linearization one obtains Kramers-Kronig-type dispersion relations between constants of seemingly different phenomena. For example, a Kramers-Kronig relation is obtained between the Verdet constant and the gain coefficient for stimulated Raman scattering by paramagnetic ions in a large dc magnetic field. The effective Hamiltonian is explicitly evaluated from some illustrative examples and its general phenomenological form for a paramagnetic ion in cubic symmetry is written down and discussed.

### 1. INTRODUCTION

THE application of high-intensity laser radiation to various materials has resulted in observation of new effects which arise from the nonlinear response of

media to optical-frequency fields.<sup>1</sup> A number of authors<sup>2-4</sup> have discussed different nonlinear optical effects phenomenologically in terms of a potential function  $F$ , whose derivatives with respect to various fields

\* This work was supported in part by the Joint Services Electronics Program (U. S. Army, U. S. Navy, and U. S. Air Force) under Contract Nonr-1866(16), and by the Division of Engineering and Applied Physics, Harvard University.

† Alfred P. Sloan Research Fellow.

‡ Present address: Bell Telephone Laboratories, Murray Hill, New Jersey.

<sup>1</sup> These effects are reviewed by N. Bloembergen, *Nonlinear Optics* (W. A. Benjamin Inc., New York, 1965), or P. S. Pershan, *Progress in Optics*, edited by E. Wolf (to be published), Vol. V.

<sup>2</sup> D. A. Kleinman, *Phys. Rev.* **126**, 1977 (1962).

<sup>3</sup> J. A. Armstrong, N. Bloembergen, J. Ducuing, and P. S. Pershan, *Phys. Rev.* **127**, 1918 (1962).

<sup>4</sup> P. S. Pershan, *Phys. Rev.* **130**, 919 (1963).